Ignition Suppression by CF_3Br and CF_3I of $H_2/O_2/Ar$ Mixtures: Detailed Studies of Time and Space Resolved Radical Profiles

A. McIlroy

The Aerospace Corporation
Mechanics and Materials Technology Center
P. O. Box 92957/M5-754
Los Angeles, California 90009-2957

Introduction

While steady progress continues toward the goal of finding halon replacements, the urgency of the problem has led to empirical searches which often neglect, out of necessity, the fundamental physics and chemistry of fire suppression and inhibition. Although a variety of halon replacements is or soon will be commercially available, their performance in terms of fire suppression is typically a factor of two worse than that of the halons they replace. The requirements for the halon replacements are smngent and often conflicting: high fire suppression performance, low toxicity, low reactivity and environmental acceptability. Two of these performance requirements, fire suppression and environmental acceptability, are particularly difficult since the same halogen radicals that catalytically inhibit combustion also catalytically destroy stratospheric ozone. Since strict regulations now drive environmental compliance, it is not surprising that a significant research effort has been devoted to elucidating the environmental issues of stratospheric ozone depletion and global warming, and that thus fire suppression performance might have to be sacrificed for environmental compliance. In order to achieve simultaneously fire suppression performance greater or equal to the halons and environmental acceptability, we will need an understanding of fire suppression that rivals the detailed chemical and physical knowledge-base developed for the problem of stratospheric ozone depletion.

A complete understanding of fire suppression and inhibition will require a wide range of investigations. Both theoretical and experimental studies are needed to develop chemical reaction mechanisms, to measure missing reaction rates, to develop models coupling chemistry and gas dynamics, and to validate these models through carefully designed experiments. Here we seek to address primarily this last point. In contrast to ozone depletion, fire suppression is in some ways easier to study since realistic model scenarios can be studied under controlled, laboratory conditions. In recent years, a great deal of effort has been expended to develop flame diagnostic techniques to probe in detail the physics and chemistry of combustion. In particular, laser based diagnostics offer the ability to

probe a wide variety of flame properties with high spatial and temporal resolution and without perturbing the flame. A wide variety of techniques have been employed including laser induced fluorescence, Raman scattering and absorption spectroscopy.[1] To date these techniques have been largely unexploited in fire suppression research.

Here we describe a study utilizing time-resolved, planar laser induced fluorescence (PLIF) imaging[2] to study laser-spark ignited gas mixtures. This PLIF imaging technique provides species concentration data with time and spatial resolution of $<1\,\mu s$ and $<100\,\mu m$ respectively. By using a laser-induced spark as an ignition source, we eliminate the possibility of perturbations due to surfaces (e.g. electrodes) of the ignition source, control the energy, spatial extent and position of the ignition source, and provide excellent optical access for the PLIF technique. Previous and ongoing studies provide detailed insight into the mechanism of laser-spark ignition.[3,4,5] This experimental approach has the advantage that observation can be made for both ignitable and fully suppressed gas mixtures. Thus models can be tested over a wider range of conditions than in experiments that rely on a steady-state, ignited flame.

In this contribution, we present PLIF images of hydroxyl radical concentration profiles for ignition attempts in hydrogen/oxygen/argon mixtures doped with the halon 1301, CF_3Br, and a proposed high-performance replacement, CF_3I. This is a particularly compelling comparison since the most detailed previous fire suppression studies used halon 1301[6,7,8,9] and led in part to Westbrook's development of a detailed suppression reaction model for halon 1301.[10] To first order, we may assume that this mechanism is valid for all CF_3X species. The simple substitution of iodine for bromine will provide an excellent test of the generality of this reaction mechanism. Furthermore, iodides are the only class of compounds identified so far that combine environmental acceptability with fire suppression performance comparable to the halons.

The H_2/O_2 combustion system is chosen for several reasons. First, hydrogen fires pose a significant safety hazard in a variety of industrial settings including semiconductor manufacturing and space launch sites. Second, this combustion system is well described by a relatively simple reaction mechanism. Thus it should be feasible to develop practical, yet sophisticated models that combine chemistry and hydrodynamics in a realistic matter. Third, inhibition and suppression of hydrogen fires has historically proven quite difficult. The halons which are excellent hydrocarbon fire suppressants have poor performance in hydrogen fires. With the requirement for new fire suppressants, this is a excellent time to revisit this problem with modem analytical techniques.

Experimental

The laser-spark ignition, planar laser induced fluorescence (PLIF) imaging apparatus (see Figure 1) has been described in detail elsewhere and only a brief description is included here.[5] A pulsed Nd:YAG laser (22 mJ/pulse, 8 ns duration) is focused to create an isolated spark 1.0 cm above an open-air bumer located beneath an exhaust hood. Gas flow through the burner is controlled by a set of mass flowmeters calibrated against a standard flowmeter for each gas or mixture in use. At a variable delay after the ignition pulse, the expanding flame kernel is probed by a frequency doubled dye laser (2 mJ/pulse at 285 nm or 355 nm, 7 ns duration) shaped into a sheet 2 cm x 250 μm with a one dimensional telescope. For the CF_3Br experiments, the laser is tuned to the Q1(5) line in the (1.0) vibrational band of the $A^2\Sigma^+ \leftarrow X^2\Pi$ transition in OH. However, 285 nm light strongly photodissociates CF_3I to produce CF3 + I. For the CF_3I experiments, the laser is instead tuned to the P1(5) line in the (0,0) vibrational banh of the $A^2\Sigma^+ \leftarrow X^2\Pi$ transition in OH. The laser power is also reduced to 0.5 mJ to minimize the increased scattered light contribution due to resonant detection, Precise tuning of the dye laser is accomplished by maximizing the OH laser induced fluorescence (LIF) from a small natural gas flame. An intensified, uv sensitive ccd camera system aligned parallel to the sheet of laser light observes OH $A^2\Sigma^+ \leftarrow X^2\Pi$ (0.0) (CF_3I) and (1.1) (CF_3Br) band PLIF signal through a 308 nm bandpass filter. Since the initial description of the apparatus, the camera objective lens has been upgraded from a simple system consisting of two spherical lenses to a uv grade, achromatic, f/4.5, complex six element uv/Nikor camera lens to improve image quality and sensitivity.

All experiments described here are carried out with a gas mixture of 10%H_2 in an "artificial air" mixture of 20% O_2 in Ar. The use of Ar rather than N_2 gas as the diluent simplifies modeling efforts by rigorously eliminating the need to include nitrogen chemistry. The initial temperature and pressure are 295 K and 760 torr respectively. The flow velocity through the bumer is 10.4 cm/s. In the previous study,[5] a secondary flow of Ar through the outer shield ring was used to eliminate the possibility of shear effects at the edge of the central burner flow. Comparisons of experimental results with and without shroud gas have shown that for our ignition experiments which are confined to the central 2 cm of the 6 cm diameter burner, the shroud flow is unnecessary. The CF_3X is added to the $H_2/O_2/Ar$ flow in the mixing manifold and is controlled by a calibrated mass flowmeter.
The data set described here utilizes laser-sparks of 16.5-18.5 mJ measured as described previously. These spark energies are well above the minimum ignition energy for a 10% H_2/air mixture.

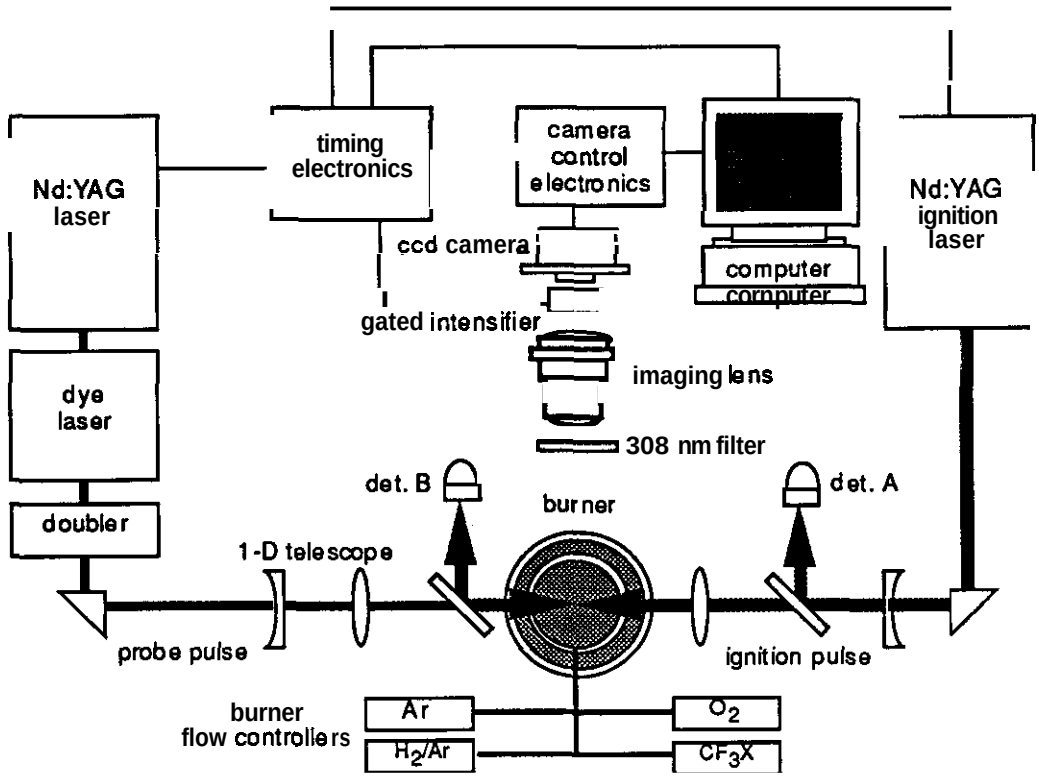

Figure 1: Experimental apparatus.

Results

To facilitate comparisons between existing and candidate fire suppressants, we have taken time-resolved PLIF images of hydrogen ignition in the presence of halon 1301, one of the two most common halons. PLIF images of OH have been obtained as a function of delay after the laser-induced spark in mixtures of 10% hydrogen in artificial air consisting of 21% oxygen in argon doped with 0%, 4% (Figure 2) and 8% (Figure 3) halon 1301. The 4% 1301 image series in Figure 2 shows behavior typical of an igniting flame kernel. At short times ($t<100\mu s$), a toroidal shape dominates the kernel geometry. As we[5] and others have shown," the toroidal geometry is due the rapid deposition of energy into the spark by the nanosecond timescale laser pulse. This structure is also commonly observed in fast ($t<1\ \mu s$) electric discharge sparks.[12] Although the toroidal shape is intriguing, its presence is independent of ignition and so is not a focus of this study. At later times, a flame front develops and propagates to the left in Figure 2, back toward the focusing lens for the spark laser. This extremely anisotropic propagation is a unique feature of laser spark ignition.[5,11] Like the toroidal shape at short times, this anisotropic flame propagation results from the initial flow field generated by the laser-induced spark. The kernel of the spark is formed by nonresonant multiphoton ionization of the gas. This ionized plasma

then heats the surrounding gas, ionizing a small portion. The gas on the laser side can then preferentially absorb more laser light through the inverse Bremsstrahlung process further heating and ionizing it. This process continues throughout the laser pulse building up the spark back along the path of the spark laser. The rapid growth of the spark produces a high velocity transport wave in the direction of spark expansion.[13,14] The damped remnants of this wave are believed responsible for the asymmetric flame propagation.5 By 2.00 ms, the toroidal shape is lost, and the dominate feature is the flame front. Flame front survival beyond 2 ms is indicative of successful ignition

In contrast to the igniting 4% halon 1301 images, the 8% halon 1301 images in Figure 3 show strikingly different behavior. Again, at early times the dominant feature is the toroidal geometry. However, the intensity of the OH fluorescence is significantly lower even at a delay of only 100 μs. Note that both Figure 2 and 3 are plotted on the same scale to facilitate comparison. Other differences are immediately evident; in the 100 μs panel of Figure 2, only the two large lobes of the toroid are present whereas in the 100 μs panel of Figure 3 there are four prominent peaks. Even at this short time, the 8% flame kernel shows evidence of breaking up. At a delay of 300 μs, a weak flame front appears as a series of nearly disconnected peaks. However, this flame front rapidly dissipates and has extinguished at the 600 μs delay leaving only remnants of the torus. Clearly 8% halon 1301 is sufficient to suppress flame formation in the 10% hydrogen/"air" mixture.

Similar images are observed for the addition of 4% and 8% CF_3I to the 10% hydrogen/"air" mixture. Again weak flame propagation is observed for the mixture containing 4% CF_3I and the flame is inhibited for the 8% mixture. This suggests that the performance of CF_3I is comparable to halon 1301 for hydrogen ignition suppression. This is in good agreement with previous investigations that have shown similar performance for these two agents in hydrocarbon applications.[15,16]

Although the overall performance may be similar for halon 1301 and CF_3I, our data indicate that their behavior is not identical. These differences are most clearly seen in by comparing the total OH PLIF signal as a function of time for the different mixtures. Figure 4 shows the integrated OH PLIF signals for the time points and suppressant concentrations investigated. The curve labeled "No Suppressant" is for a fully igniting, 10% H_2/"air" mixture. It shows a rapid rise in OH intensity as the flame kernel grows followed by a leveling off as flame propagation begins. Although the 4% 1301 mixture ignites, the time dependence of the integrated PLIF signal is quite different. Instead of a steady rise in PLIF intensity, this mixture shows an initial rise followed by a steep decline in the first 1000 μs. The flame front then propagates, but with a total intensity reduced from the unsuppressed

case. The 8% 1301 curve also shows an induction period in which substantial OH is formed before the flame kernel is fully suppressed.

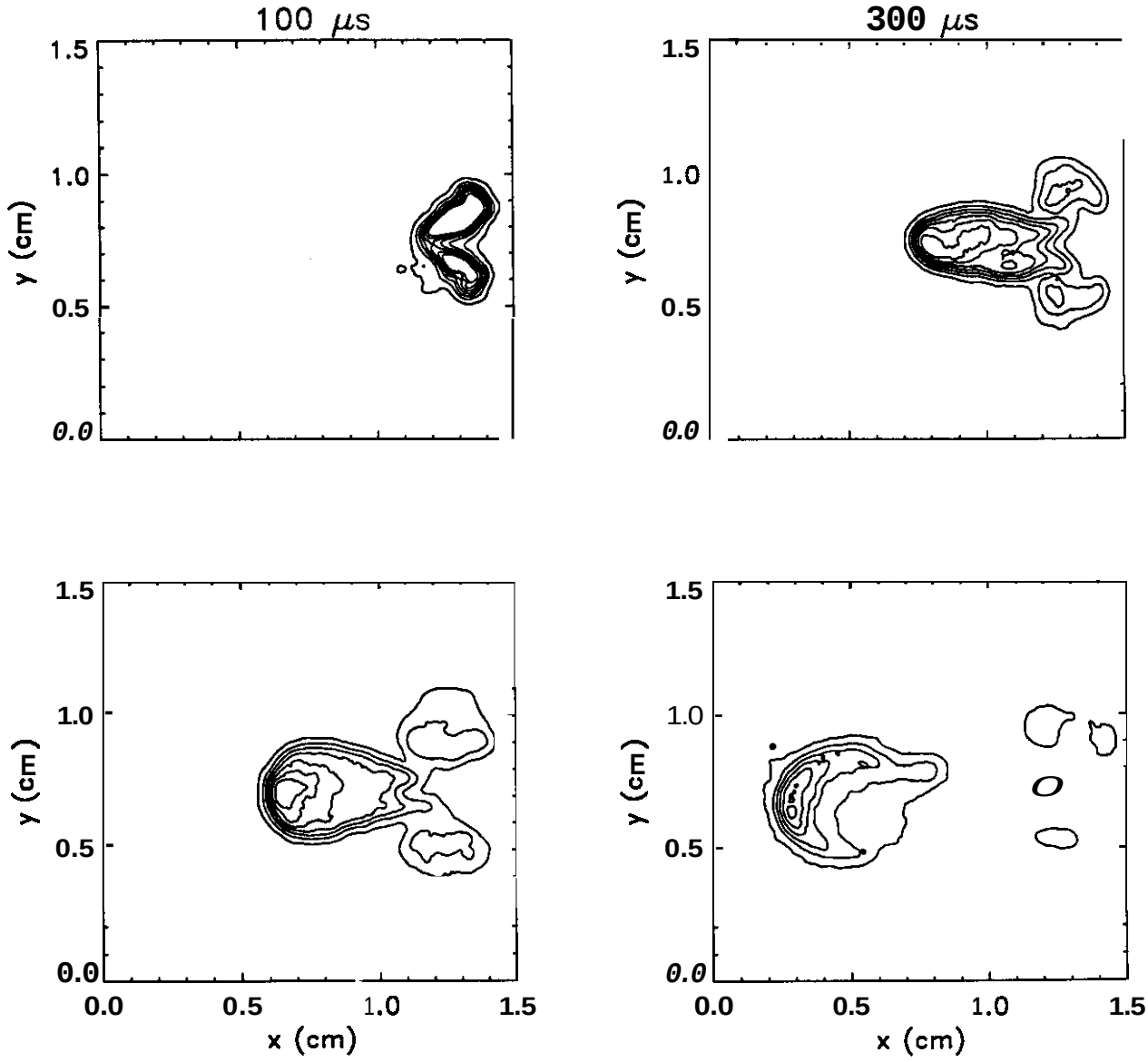

Figure 2: Contour plots of OH PLIF images at selected delays after laser-spark ignition in mixtures containing 4% halon 1301, 10% hydrogen and balance artificial air consisting of 21% oxygen in argon. The ignition laser enters from the left and is focused at approximately 1.3 cm on the x-axis and 0.75 cm on the y-axis. The short time flame kernel images ($t \leq 300$ μs) show evidence of the toroidal geometry produced by a short duration spark. As time progresses, the dominant feature becomes the formation of a flame front that propagates backward along the spark laser path. This effect is unique to laser-induced spark ignition. Although hydrogen flames still propagate in 4% halon 1301, suppression is evident in the overall reduction of OH fluorescence intensity (see Figure 3).

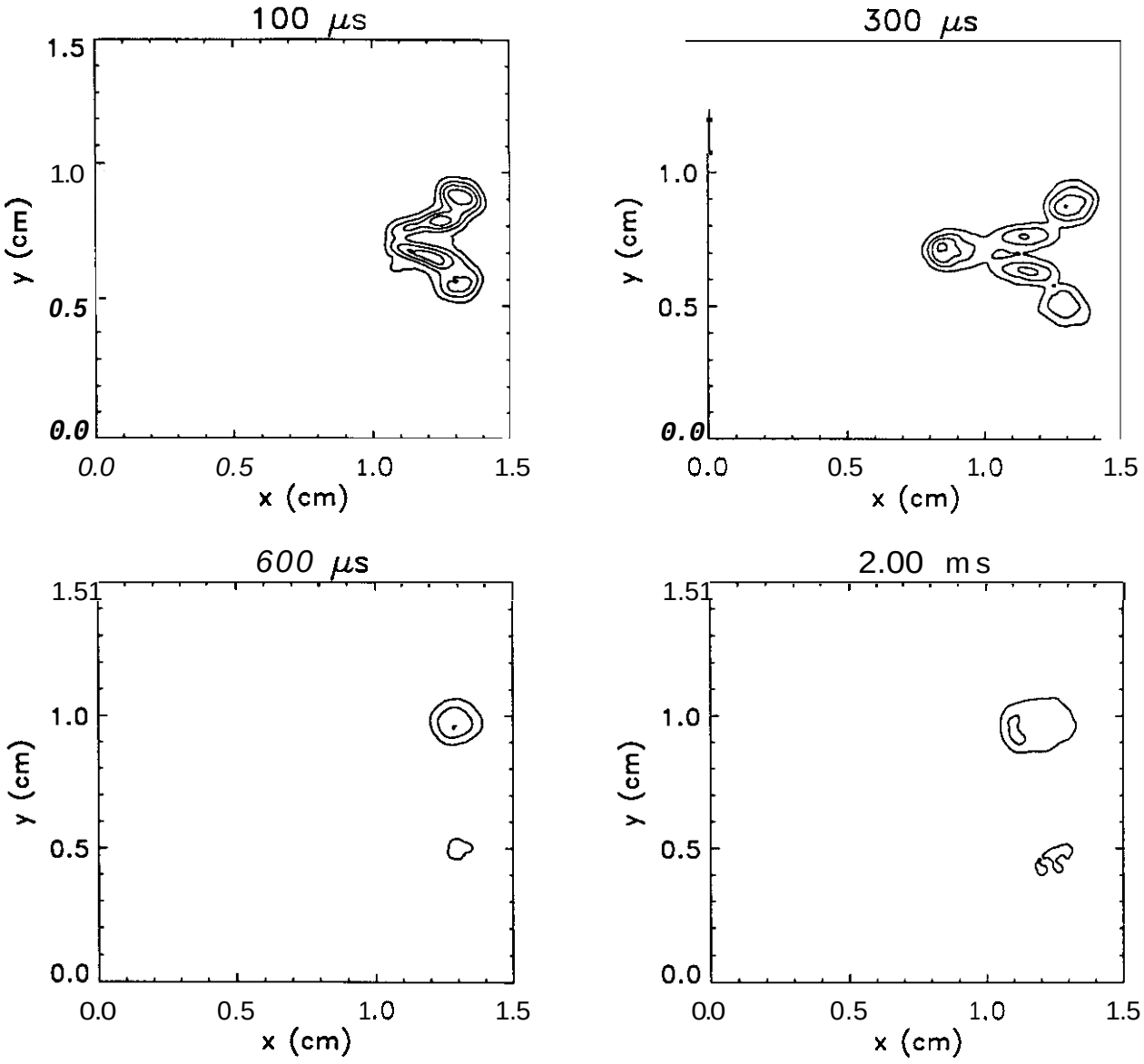

Figure 3: Contour plots of PLIF images of OH at selected delays after laser-spark ignition in mixtures containing 8% halon 1301, 10% hydrogen and balance artificial air consisting of **21%** oxygen in argon. The ignition laser enters from the left and is focused at approximately 1.3 cm on the x-axis and 0.75 cm on the y-axis. Unlike the series of images shown for the **4%** halon 1301 ignition attempts, no sustainable flame front develops and the initial flame kernel is essentially extinguished by 2.00 ms after the spark. At early times although the overall shape of the kernel is similar to that for ignitable images, the kernels are fragmented and already show signs of extinguishment.

In contrast, the curves for the CF_3I doped ignitions show no induction period, but instead display only a smooth rise or fall in OH intensity. The zero offset for the 8% CF_3I mixture is not an indication of flame propagation, but rather is due to the formation of more

OH in the torus region. This may be the result of higher spark energies due to more efficient absorption of the spark-laser energy by CF_3I.

Discussion

In order to better understand the fire suppression performance of CF_3I in comparison to CF_3Br, we have begun a program of ignition modeling employing detailed chemical mechanisms. We describe here the results from a preliminary thermal ignition model which employs premixed gases under constant pressure, adiabatic conditions. Although our experimental conditions are very different, these models do provide some insight into the chemical kinetic differences between CF_3I and CF_3Br and suggest an explanation for the time dependence of the **OH** intensity profiles. Since in any real combustion system, the suppression characteristics are dependent on both chemical kinetic and gas transport properties, we are currently developing a more sophisticated model which includes one dimensional gas transport and thus more closely approximates our experimental results.

Although the model described here neglects transport effects, it does employ a complex reaction mechanism of 52 reactions to describe the hydrogen/oxygen combustion in the presence of a CF_3X fire suppressant. The hydrogen combustion mechanism and reaction rates are those of Thorne ef *al.*[17] while the halon chemistry is taken from Westbrook.[10] For halon 1301, we use the reaction rates of Westbrook.[10] For CF_3I, we use the CF_n[10] and HI chemistry from Westbrook.[18] The missing reaction rates constants for the reactions

$$CF_3I \rightarrow CF3 + I$$
$$H + CF_3I \rightarrow HI + CF_3$$
$$I + CF_3I \rightarrow I_2 + CF3$$

necessary for the implementation of Westbrook's halon suppression mechanism are taken from Zaslonko *et. al.*,[19] Moms *et. al.*[20] and Skorobogatov *er al.*[21] respectively. We utilize the CHEMKIN chemical kinetics subroutine package to implement the calculations.[22] Using data from the JANAF Thermochemical Tables,[16,23] we have augmented the standard thermodynamic database included with CHEMKIN to include the necessary halogenated compounds. The initial conditions employed are as follows: 1 atm pressure, 1000 K temperature, stoichiometric mixture of hydrogen in artificial air consisting of 21% oxygen in argon, varying suppressant concentrations.

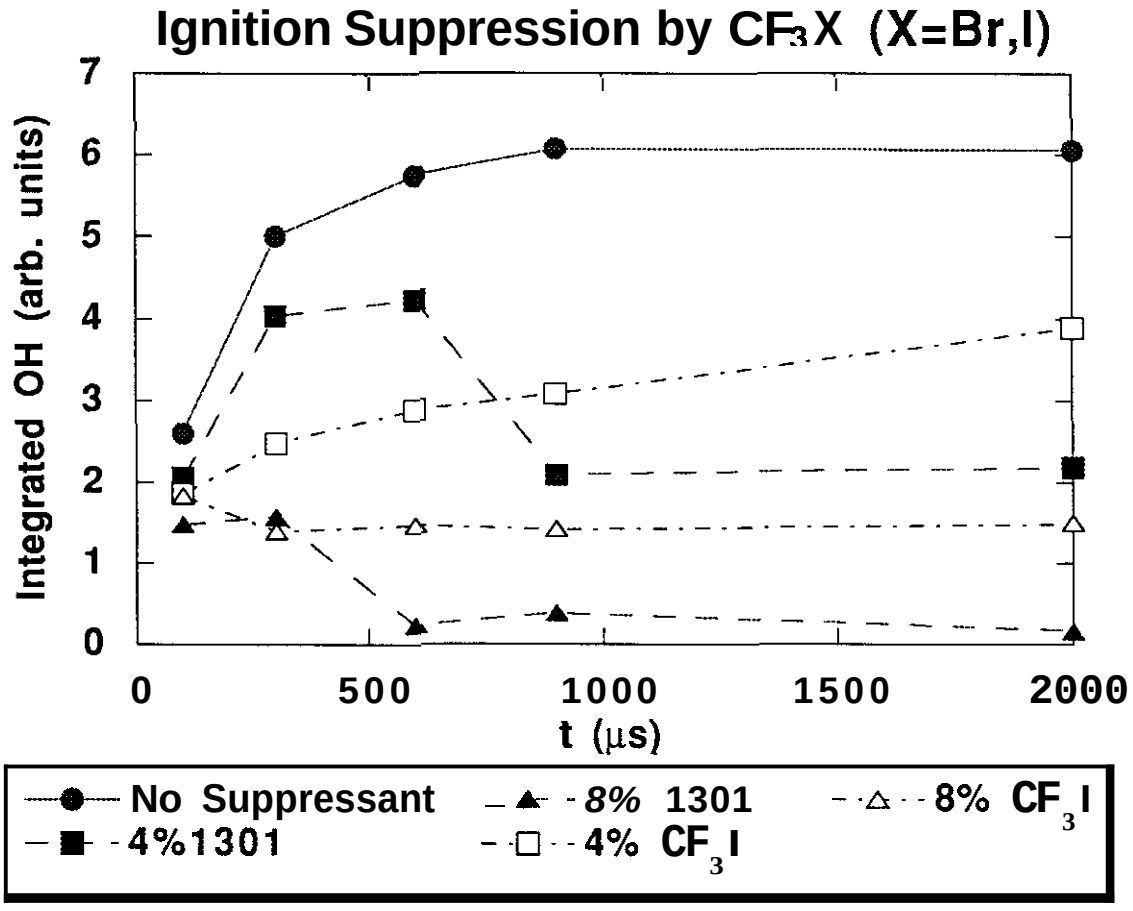

Figure 4: Time dependence of integrated OH fluorescence from PLIF images of ignition attempts in halon 1301 and CF_3I doped mixtures of 10% hydrogen and balance artificial air consisting of 21% oxygen in argon. The "No Suppressant", 10% H_2/artificial air mixture is fully ignited by the laser spark. The "8% 1301" mixture flame front has lost coherence by 600 μs and is extinguished by 2.00 ms. The "8% CF_3I" mixture shows some intensity at long times, but it is localized in the initial spark region and is not characteristic of a propagating flame. The "4% 1301" and "4% CF_3I" mixtures represents intermediate cases of partial suppression.

The initial temperature of 1000 K is sufficient to ignite a stoichiometric H_2/O_2 mixture after a short delay of approximately 200 μs. Ignition is observed as a sudden rise in temperature and conversion of products to reactants. With the addition of a suppressant, CF_3Br or CF_3I, the ignition delay increases as shown in Figure 5. Clearly the ignition delay rises much faster for CF_3I than CF_3Br indicating that based on chemistry alone the iodide should be a superior fire suppressant. Previous comparisons of bromine versus iodine suppression with HX and CH_3X, X=Br, I, have also noted that based on chemistry alone iodine containing compounds should be superior fire suppressants to the analogous bromine compounds.[15,16] However, experimental results show comparable performance with a slight edge to the bromine compounds.[24] As other studies have suggested, this

discrepancy may be due to transport effects. To date, no effects directly attributable to these rate differences have been observed.

Our results show an induction period before suppression for CF_3Br, but not CF_3I. The induction period may be due to the difference in chemical reaction rates between these species. Specifically, previous models have shown that the suppression cycle is dependent on X and HX species, not the stable precursor CF_3X. If unimolecular decomposition of CF_3X is slow compared to initial flame growth, this could lead to an induction period before suppression. At typical flame conditions of 1500 K and 1 atm, our model indicates that CF_3I has a lifetime of **5.5** μs and CF_3Br has a lifetime of **69 ps.** At lower temperatures this difference increases and the timescales approach the observed induction **period** of ~600 μs for CF_3Br, but remains more than a factor of ten faster for CF_3I. On the timescales probed in these experiments, these results are consistent with the observation of **an** induction period for the bromine compound, but not the iodide. Thus the difference in these induction periods for CF_3Br and CF_3I may be attributable to differences in the chemical reaction rates.

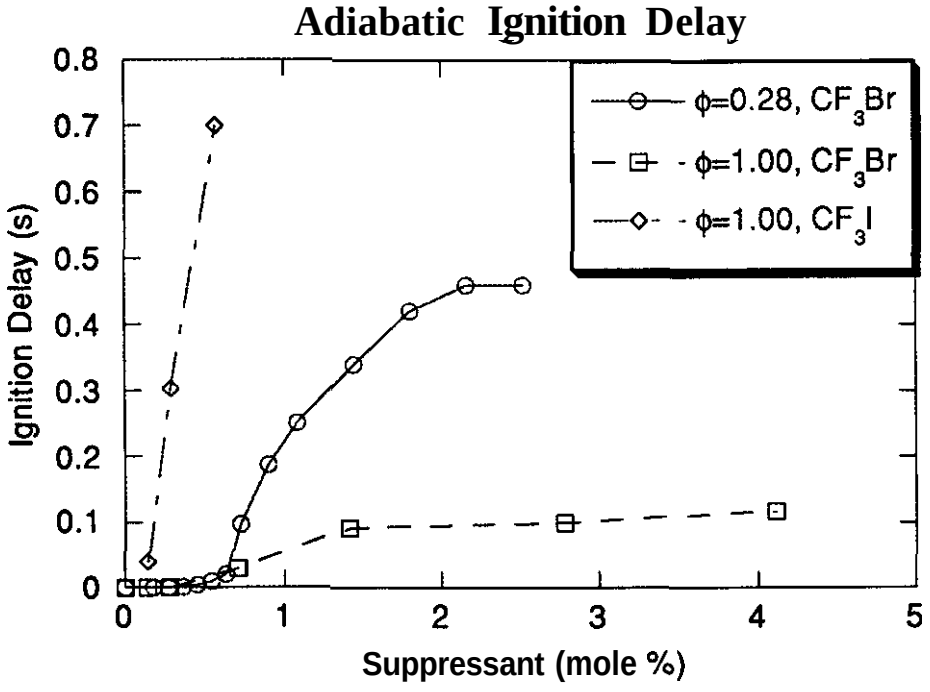

Figure **5:** Calculated ignition delay times for $H_2/O_2/CF_3X$ suppressant model. Constant pressure, adiabatic conditions are assumed with initial temperature of 1000 K and pressure of 1 atm See text for details of model.

Conclusions

We have shown that PLIF imaging has the potential for providing a detailed diagnostic of ignition suppression under conditions of partially and fully suppressed flames. The performance of CF_3I and CF_3Br appear to be comparable for the hydrogen/oxygen combustion system studied. However, difference are observed in the time dependence of the flame kernel development. An induction period before suppression is observed for the bromine compound, but not the iodine compound. The timescale for the induction period is suggestive of CF_3Br unimolecular decay which produces the active suppression species. This process is more than an order of magnitude faster for CF_3I and would not lead to an observable induction period on the timescales investigated here.

Acknowledgments

Financial support for this work was provided in part by the Aerospace Sponsored Research program. The author would like to thank Dr. Jack Syage, Dr. Brian Brady and Dr. Ronald Cohen of the Aerospace Corporation and Prof. Paul Ronney at the University of Southern California for several helpful discussions.

References

[1]For a review of laser combustion diagnostics see Eckbreth, A. C., *Laser Diagnosticsfor Combustion Temperature and Species,* Abacus Press, Cambridge, 1988.

[2]For a review of this technique see J. M. Seitzman and R. K. Hanson, "Chapter Six: Planar Fluorescence Imaging in Gases" in *Instrumentation for Flows with Combustion,* Academic Press, Orlando, 1993.

[3]For a review of laser versus electric spark ignition see Ronney, P. D., *Proc. SPIE - Int. Soc. Opt. Eng.* 1862:2 (1993).

[4]Syage, J. A., Fournier, E. W., Rianda, R., and Cohen, R. B., *J. Appl. Phys.* 64:1499 (1987).

[5]T. A. Spiglanin, A. McIlroy, E. W. Fournier, R. B. Cohen, and J. A. Syage, *Combustion and Flame,* submitted.

[6]J. C. Biordi, C. P. Lazzara and J. F. Papp, U. S. Bur. Mines Rept. of Investigations RI8029 (1975).

[7]J. C. Biordi, C. P. Lazzara and J. F. Papp, *Fifteenth Symposium (International) on Combustion,* The Combustion Institute, Pittsburgh, PA, 1975, p. 917.

[8]J. C. Biordi, C. P. Lazzara and J. F. Papp, *J. Phys. Chem.* 81:1139 (1977).

[9]J. C. Biordi, C. P. Lazzara and J. F. Papp, *J. Phys. Chem.* 82:125 (1978).

[10]C. K. Westbrook, ***Combustion Science and Technology*** 34201 (1983).

[11]Seitzman, J. M., Paul, P. H., and Hanson, R. K., Paper 88-2775, AIAA Thermophysics, Plasmadynamics and Lasers Conference, San Antonio, TX, 1988.

[12]Kono, M., Niu, K., Tsukamoto, T., and Ujiie, Y., ***Twenty Second Symposium (International)on Combustion,*** The Combustion Institute, Pittsburgh, 1988, p. 1643.

[13]C. DeMichelis, ***IEEE J. Quantum Electronics QE-5,*** 188 (1969).

[14]S. A. Ramsden and W. E. R. Davies, ***Phys. Rev. Lett.*** 13,227 (1964).

[15]C. K. Westbrook, ***Nineteenth Symposium (International) on Combustion,*** The Combustion Institute, Pittsburgh, 1982, p. 127

[16]Lerner, N. R., Cagliostro, D. E., ***Combustion and Flame*** 21:315 (1973).

[17]Thorne, L. R., Branch, M. C., Chandler, D. W., Kee, R. J., and Miller, J. A., ***Twenty-First Symposium (International) on Combustion,*** The Combustion Institute, Pittsburgh, 1986, p. 965.

[18]C. K. Westbrook, ***Combustion Science and Technology*** 23:201 (1980).

[19]Zsalonko, I. S., Mukoseev, Yu. I., Skorobogatov, G. A., Slinkin, S. V., ***Kinet. Catal.*** 27:636 (1986).

[20]Morris, R. A., Donohue, K., McFadden, D. L., J. Phys. Chem. 93:1358 (1989).

[21]Skorobogatov, G. A., Dymov, B. P., Khripun, V. K., ***Kinet. Catal.*** 32:220 (1991).

[22]Kee, R. J., Rupley, F. M., and Miller, J. A., Sandia Report, SAND89-8009.UC-401, 1989.

[23]Chase,Jr., M. W., Davies, C. A., Downey, Jr., J. R., Frurip, D. J., McDonald, R. A., and Syverund, A. N., ***JANAF Thermochemical Tables Third Edition,*** American Chemical Society, New York, 1985.

[24]Sheinson, R. S., Penner-Hahn, J. E., Indritz, D., ***Fire Safety Journal,*** 15:437 (1989).